TISSUE ENGINEERING: Part A
Volume 21, Numbers 11 and 12, 2015

DOI: 10.1089/ten.tea.2014.0573

Recellularization of Rat Liver Scaffolds by Human Liver Stem Cells

Victor Navarro-Tableros, MD, PhD,[1] Maria Beatriz Herrera Sanchez, PhD,[1] Federico Figliolini, PhD,[1] Renato Romagnoli, MD,[2] Ciro Tetta, MD,[3] and Giovanni Camussi, MD, PhD[4]

In the present study, rat liver acellular scaffolds were used as biological support to guide the differentiation of human liver stem-like cells (HLSC) to hepatocytes. Once recellularized, the scaffolds were maintained for 21 days in different culture conditions to evaluate hepatocyte differentiation. HLSC lost the embryonic markers (alpha-fetoprotein, nestin, nanog, sox2, Musashi1, Oct 3/4, and pax2), increased the expression of albumin, and acquired the expression of lactate dehydrogenase and three subtypes of cytochrome P450. The presence of urea nitrogen in the culture medium confirmed their metabolic activity. In addition, cells attached to tubular remnant matrix structures expressed cytokeratin 19, CD31, and vimentin. The rat extracellular matrix (ECM) provides not only a favorable environment for differentiation of HLSC in functional hepatocytes (hepatocyte like) but also promoted the generation of some epithelial-like and endothelial-like cells. When fibroblast growth factor–epidermal growth factor or HLSC-derived conditioned medium was added to the perfusate, an improvement of survival rate was observed. The conditioned medium from HLSC potentiated also the metabolic activity of hepatocyte-like cells repopulating the acellular liver. In conclusion, HLSC have the potential, in association with the natural ECM, to generate *in vitro* a functional ''humanized liver-like tissue.''

Introduction

ABOUT 170 MILLION people worldwide are affected by chronic liver diseases eventually progressing to fibrosis and in several cases culminating in cirrhosis.[1] Liver transplantation is the only efficient treatment that radically improves the outcome of liver failure. However, the accessibility of whole livers for transplantation is limited by the number of donors. Furthermore, the transplants of mature hepatocytes or hepatocytes obtained by neonatal livers are considered potential candidates for transplantation as an alternative therapy. Nevertheless, the availability of organs for isolation of mature hepatocytes as well as the difficulty to expand them *in vitro* are the main limitations to their use.[2]

Recently, researchers focused on stem/progenitor cells as a potential strategy for treatment of acute or chronic liver diseases. Stem cells (SC) are characterized by a self-renewal capacity and possess a high potentiality to differentiate in diverse cell progeny. The generation of mature hepatocytes from SC could offer an alternative for treatment of liver diseases and for correction of genetic disorders of liver metabolism. Embryonic stem cells (ESC) have been extensively studied for their potential to differentiate into different hepatic cell phenotypes.[3,4] However, the formation of teratoma has been observed in the liver and other organs after ESC transplantation in mice.[5,6]

Therefore, alternative sources of human SC have been explored. At present, bone marrow mesenchymal stem cells (BM-MSC) are preferred for potential clinical applications as they have some advantages related to their commitment to hepatic lineage.[7–13] Adult human liver stem-like cells (HLSC) isolated by our group may represent an alternative for regenerative medicine because they are easily expandable.[14,15] HLSC have multiple differentiating capabilities distinct from those of oval SC. They express several mesenchymal, but not hematopoietic, stem cell markers and express embryonic markers such as alpha-fetoprotein (AFP), nestin, nanog, sox2, Musashi1, Oct 3/4, and pax2.[14,16] Moreover HLSC express albumin, AFP and cytokeratin 18 (CK18) supporting their partial hepatic commitment.[14] The effectiveness in restoring the hepatic mass and function has been also described.[16] Indeed, HLSC are able to enhance survival and to improve the tissue recovery in SCID mice with fulminant liver failure. These characteristics make the HLSC potential candidates for generation of functional hepatocytes to be used in regenerative medicine.

[1]Translational Center for Regenerative Medicine and Molecular Biotechnology Center, University of Torino, Torino, Italy.
[2]Liver Transplantation Center, University of Torino, Torino, Italy.
[3]EMEA LA Medical Board, Fresenius Medical Care, Bad Homburg, Germany.
[4]Department of Medical Sciences, University of Torino, Torino, Italy.

The dream in regenerative medicine is to develop strategies to reconstitute whole organ morphology and to reestablish its function. To promote a regeneration of a functional organ, it is not only necessary to generate tissue-specific cells but it is also important to recreate the micro- and macroenvironments critical for cell structural organization and function. Currently, the efforts of researchers are directed to design synthetic scaffolds to mimic the macro- and microstructure of tissues that favor vascular network formation.[17–20] Alternative strategies such as the coseeding with endothelial cells to promote the spontaneous formation of capillary-like networks have been used.[21] Incorporation of angiogenic peptides and growth factors into synthetic scaffolds has also been attempted to promote angiogenesis within engineered tissues.[22–25] Nevertheless, in these synthetic scaffolds, the vessel connectivity to host circulatory system is incomplete and restricted to the scaffold edges when they are transplanted.[26]

To solve these difficulties, natural scaffolds with intact tridimensional anatomical architecture have been successfully used recently for different organs, including the liver.[27] The natural extracellular matrices (ECMs) provide some advantages over the synthetic scaffolds. ECMs have the complex composition of bioactive molecules and lack immunoreactivity,[28] offer the type-specific niches necessary for cell engraftment, and are also able to regulate the cellular behavior and functionality.[29]

In this respect, the generation of natural liver bioscaffolds may offer the tridimensional mechanical support for a favorable cell engraftment and commitment. Moreover, natural liver bioscaffolds may allow optimal delivery of nutrients and offer an appropriate environment for regeneration of a fully functional organ.

In this study, we explored the potential of rat acellular liver bioscaffolds to promote differentiation of HLSC into mature hepatocytes and into other nonhepatocyte cells. We also explored the contribution of different culture conditions in improving the maturation of hepatocyte-like cells. Finally, we analyzed the capacity of hepatocyte-like cells to modify their micro- and macroenvironment, substituting the native rat ECM with the human counterpart.

Materials and Methods

Animals

Young male Wistar rats (250–300 g) were obtained from the local animal facility. Animal studies were approved by the local ethic committee and conducted in accordance with the National Institute of Health Guide for the Care and Use of Laboratory Animals. Animals were sacrificed by cervical dislocation.

Isolation, characterization, and culture of HLSC

HLSC were isolated from human cryopreserved normal hepatocytes obtained from Lonza and were cultured and characterized as previously described.[14] Specifically, HLSC were cultured in a standard culture medium containing a 3:1 proportion of α-minimum essential medium and endothelial cell basal medium-1, supplemented with L-glutamine 2 mM, penicillin 100 IU/mL/streptomycin 100 μg/mL, and 10% fetal calf serum (α-MEM/EBM/FCS; Gibco/Cambrex) and maintained in a humidified 5% CO_2 incubator at 37°C. Cells up to ≈ 80% confluence are trypsinized and harvested by centrifugation at 1200 rpm for 5 min. HLSC at passages 3 to 7 and ≈ 80% of confluence were used in all the experiments. By confocal microscopy and FACS analysis, HLSC expressed several embryonic markers (AFP, nestin, nanog, sox2, Musashi1, Oct 3/4, and pax2), MSC (CD29, CD73, CD44, and CD90), and the hepatic marker albumin as previously described.[14]

Preparation of HLSC-derived conditioned medium

The HLSC-derived conditioned medium (HLSC-CM) was obtained as described previously by our group.[30] Briefly, supernatants of HLSC cultured in α-MEM/EBM/FCS were collected after 24 h. After centrifugation at 3000 *g* for 10 min to remove cell debris, cell-free supernatants were concentrated ~25-fold by centrifugation at 2700 *g* for 75 min, using Ultra-PL 3 ultrafiltration units (Amicon-Millipore) with a 3-kDa molecular weight cutoff and stored at −20°C until its use.

Generation of acellular liver scaffolds

After cervical dislocation, a longitudinal abdominal incision through the midline was performed, and all three inferior vena cava (IVC), portal vena, and the cystic duct (CD) were cannulated using 22G or 24G cannulas (as appropriate) and ligated proximally with a silk nonabsorbable surgical suture 6-0 (Ethicon; Johnson-Johnson Intl.). Connecting a 10-mL syringe to the cannulas, 1 mL of phosphate-buffered saline (PBS) containing 1 IU/μL of heparin (Epsoclar 25.000 IU/5 mL; Hospira) was perfused through each cannula to prevent coagulation. Posteriorly, a midline sternotomy was done; the superior vena cava (SVC) was cannulated, fixed, as described above, and then perfused with a PBS-heparin solution. The liver was dissected and removed from the abdominal cavity (with its capsule intact), transferred to the perfusion camera, and connected to the Langendorff system (Hugo Sachs Elektronik-Harvard Apparatus). Then, the decellularization proceeded according to the protocol of Shupe *et al.*,[27] with some modifications. Briefly, the liver was perfused with the following: (a) PBS 1× to clear the blood (300 mL), (b) PBS solution containing different concentrations of Triton X-100 (1%, 2%, and 3%, 300 mL of each one) to disrupt the lipids of the membranes and clear most of the cellular components, and (c) 1000 mL of PBS solution containing sodium dodecyl sulfate (0.1%) to remove the remnant nuclear components containing DNA. The cannula connected to the perfusion system was changed from time to time to permit a best perfusion of the entire liver. Then, the remnant detergent was cleared from the scaffolds by perfusion with 1000 mL of PBS and sterilized with 50 mL of peracetic acid solution (PA 0.1%, ethanol 4%). Finally, scaffolds were washed with 300 mL of sterile PBS to eliminate the PA. All solutions were perfused by a peristaltic pump at 75 mmHg at a constant flow rate of 5 mL/min.

Recellularization and culture of bioscaffolds

A total of 10 mL α-MEM/EBM/FCS was perfused into the scaffolds as pretreatment, 30 min before seeding the cells to promote the best engraftment. Then, a quarter of the cell suspension was injected into the scaffolds through

Table 1. Primary Antibodies for Rat Antigens

Rat marker	*Antibody*	*Reference*	*Dilution*
Collagen IV	Rabbit polyclonal IgG	Abcam (ab19808)	1:500
Fibronectin	Rabbit polyclonal IgG	Abcam (ab23751)	1:200
Laminin	Rabbit polyclonal IgG	Abcam (ab11575)	1:200
Vimentin	Mouse monoclonal IgG1	Abcam (ab8978)	1:200
Actin	Mouse monoclonal IgG2A	Abcam (ab11003)	1:200
Cytokeratin 8-18-19	Mouse monoclonal IgG1	Abcam (ab41825)	1:100

the cannula inserted in the vena porta, whereas the other three cannulas (IVC, SVC, and CD) were clamped to avoid the efflux of the cells outside the scaffold. The same procedure was repeated by the IVC, SVC, and then by the CD.

Three different protocols were designed to explore the best one promoting cell engraftment, differentiation, and maturation: (a) only HLSC in a standard medium (hepatocyte like; $80–100 \times 10^6$ cells), (b) HLSC + 10 ng/mL epidermal growth factor (EGF)-10 ng/mL fibroblast growth factor-4 (FGF4; hepatocyte like + GF), and (c) hepatocyte like + HLSC-CM. Once cells were seeded, the bioscaffolds were cultured in static condition in a humid incubator at 37°C, air and 5% CO_2 for 21 days and the medium was changed with a fresh one every other day during the entire experiment.

Assessment of urea production

Samples of the culture medium were collected at 2, 4, 6, 14, and 21 days during the culture. The samples were centrifuged for 5 min at 1200 rpm to eliminate cellular detritus and then the supernatant was frozen at −20°C until analysis. The presence of urea nitrogen in the medium was assessed by colorimetry using a specific Human BUN Colorimetric Detection Kit (Reference K024-H1; Arbor Assays) following the instruction of the provider. The standard medium (α-MEM/EBM/FCS) was used as blank for normalization and considered as the blood urea nitrogen (BUN) concentration at time 0.

Histology

At the end of the experiments, a part of each bioscaffold was formalin fixed and paraffin embedded and 3–5 μm sections were used for histological analysis. Hematoxylin and eosin (H&E) staining was conducted by the standard method to evaluate the tissue architecture, morphology, the cell engraftment, and the organization of the hepatocyte like in the bioscaffold. Furthermore, immunocytochemistry was performed to analyze the human nature of the cells by their positivity to MHC-I human leukocyte antigen (HLA). Briefly, the endogenous peroxidase activity was blocked with 6% H_2O_2 for 10 min at room temperature. The rabbit anti-human polyclonal antibody 1:100 (HLA-1; Santa Cruz Biotechnology) was applied to slides and incubated overnight at 4°C. The next day, samples were washed thrice with PBS-Tween 0.1% for 5 min and incubated for 30 min at room temperature with the horseradish peroxidase-labeled anti-rabbit (Dako). The reaction product was developed using 3,3-diaminobenzidine. Omission of the primary antibody or substitution with the unrelated rabbit antibody served as negative control.

Table 2. Primary Antibodies for Human Antigens

Human marker	*Antibody*	*Reference*	*Dilution*
MHC class I (HLA-1)	Rabbit polyclonal IgG	Santa Cruz Biotechnology (SC-25619)	1:100
Albumin	Mouse monoclonal IgG2A	R&D Systems (MAB1455)	1:50
CytP450 1a1	Rabbit polyclonal IgG	Abcam (ab79819)	1:100
CytP450 3a4	Sheep polyclonal IgG	Abcam (ab22702)	1:100
CytP450 7a1	Rabbit polyclonal IgG	Abcam (ab65596)	1:100
LDH	Rabbit monoclonal IgG	Abcam (ab52488)	1:100
Fibronectin	Rabbit polyclonal IgG	Abcam (ab23750)	1:100
Laminin	Mouse monoclonal IgG1	Abcam (ab49726)	1:100
Vimentin	Rabbit monoclonal IgG	Abcam (ab16700)	1:100
Collagen IV	Mouse monoclonal IgG1	Abcam (ab6311)	1:100
Actin	Rabbit monoclonal IgG	Abcam (ab115777)	1:100
Cytokeratin 19	Mouse monoclonal IgG1K	Dako (M0888)	1:100
Oct 3/4	Goat polyclonal IgG	Abcam (ab14520)	1:50
AFP	Mouse monoclonal IgG1	R&D Systems (MAB1368)	1:20
Nanog	Rabbit polyclonal IgG	Abcam (ab21603)	1:100
Sox2	Rabbit polyclonal IgG	Abcam (ab15830)	1:100
Musashi1	Rabbit polyclonal IgG	Abcam (ab33251)	1:100
CD31	Rabbit polyclonal IgG	Abcam (ab28364)	1:100
Pax2	Rabbit polyclonal IgG	Covance	1:100

AFP, alpha-fetoprotein; LDH, lactate dehydrogenase.

Table 3. Secondary Antibodies

Fluorophore	*Secondary antibody*	*Reference*	*Dilution*
Alexa Fluor 488	Goat anti-rabbit IgG (H+L)	Abcam (ab11008)	1:200
Alexa Fluor 488	Goat anti-mouse IgG (H+L)	Abcam (ab11029)	1:200
Alexa Fluor 488	Donkey anti-sheep IgG (H+L)	Abcam (ab11015)	1:200
Texas Red	Goat anti-rabbit IgG (H+L)	Abcam (T2767)	1:200
Texas Red	Goat anti-mouse IgG (H+L)	Abcam (T6390)	1:200

Immunofluorescence

Immunofluorescence was performed to characterize the ECM composition and the cell phenotype. Briefly, at the end of each experiment, parts of each bioscaffold were included in Tissue-Tek-II and frozen at −80°C. Serial slides were cut longitudinally (3–5 μm) in a cryostat and fixed in acetone; then, the expression of human matrix proteins, typical markers of mature hepatocytes, and epithelial and endothelial cells were analyzed by immunofluorescence using specific antibodies (Table 2). Briefly, tissue sections were first washed with PBS 1×, incubated during 30 min at room temperature with a permeable solution containing PBS 1× and 0.25% Triton X-100, washed thrice with PBS 1× for 5 min each one, incubated for 20 min with a blocking solution containing PBS 1×, 0.1% Tween, and 0.1% bovine serum albumin (wt/vol) for 30 min at room temperature, and then incubated overnight with specific primary antibodies. For the characterization of extracellular matrix (EM) in rat acellular bioscaffolds, immunofluorescence was performed by using primary antibodies recognizing anti-rat proteins (Table 1). The expression of human markers in the HLSC recellularized bioscaffolds was analyzed by immunofluorescence using specific antibodies anti-human proteins: HLA-1, CD31, Oct 3/4, nestin; albumin, AFP, collagen IV, vimentin, cytochrome P450 1a1, cytochrome P450 3a4, cytochrome P450 7a1, lactate dehydrogenase (LDH), fibronectin, CD31, laminin, vimentin, cytokeratin 8–18, cytokeratin 19 (CK19), nanog, sox2, Musashi1, and pax2 (Table 2). Nonimmune isotypic control IgG from mouse, rabbit, or sheep was used as negative control, where appropriate. After washing with PBS-Tween solution, sections were incubated with the corresponding secondary antibodies, Alexa Fluor 488 or Texas Red, as appropriate (Table 3), washed with PBS-Tween solution, incubated for 10 min with DAPI (Dako), and after a final washing step with PBS, slides were mounted with Fluoromount (Sigma). The specificity of primary antibodies recognizing human markers was tested in acellular rat liver scaffolds or using as primary antibody, nonimmune isotypic control IgG from mouse, rabbit, or sheep, where appropriate (Supplementary Fig. S1; Supplementary Data are available online at www.liebertpub.com/tea). Microscopy analysis was performed using a Cell Observer SD-ApoTome laser scanning system (Carl Zeiss).

Analysis of differentiated cell population derived from HLSC

Ten micrographs (10× magnification) were taken for each experimental condition. The total number of cells and the number of positive cells were counted for each marker: CK19, vimentin, or CD31 and the percentage of positive cells was calculated.

Cell proliferation and apoptosis

Specimens of paraffin-fixed scaffolds were routinely processed and sectioned at 3–5 μm. Then, immunohistochemistry for detection of proliferation and apoptosis was performed as previously described[31] using the anti-PCNA monoclonal antibody (Santa Cruz Biotechnology) for proliferation or by terminal deoxynucleotidyl transferase dUTP nick-end labeling (TUNEL) for apoptosis. The percentage of positive cells was calculated as described above. Percentage of positive cells = (positive cells/total cells)*100.

Statistical analysis

Values are presented as the mean of three independent experiments in each condition ± the standard error. Data were analyzed using a *t*-test, analysis of variance (ANOVA), and Pearson's test. A probability $p < 0.05$ or 0.01 was considered significant.

Results

The macroscopic architecture was preserved in the acellular liver structures after decellularization (Fig. 1A–D). The translucent appearance of these bioscaffolds permitted to observe the presence of tubular arrangements pertaining to vessel and biliary duct remnants (Fig. 1D). The H&E staining demonstrated the absence of cells in the decellularized liver bioscaffolds (Fig. 1F) when compared with normal liver tissue (Fig. 1E). A fine fibrous network was preserved in the decellularized liver bioscaffolds. The immunohistochemical analysis showed that the remnant native ECMs contained collagen IV, cytokeratin 8–18, fibronectin, actin, laminin, and vimentin (Fig. 2A–F).

Once the acellular bioscaffolds were obtained and pretreated with a culture medium (Fig. 3A), they were recellularized with HLSC, maintained in culture for 21 days in three different conditions (see Materials and Methods section). The initial transparency of the acellular bioscaffolds allowed observing cellular distribution after infusion. By conventional microscopy, the presence of cells inside the structures was observed (Fig. 3B). The efficiency of HLSC to repopulate the rat acellular liver bioscaffolds was assessed after 21 days by H&E staining of histological preparations. We observed that cells were not only distributed throughout the matrix of the acellular liver parenchyma but also around and inside of tubular structures that seemed to belong to remnants of vessel and/or biliary duct systems (Fig. 3C). These cells were positive to the human marker HLA-1 (Fig. 3D), demonstrating their human nature and excluding their origin from rat remaining cells. No differences were observed in the different culture conditions (data not shown).

The viability of hepatocyte-like cells was maintained until the end of the experiment. The TUNEL analysis (Fig. 4),

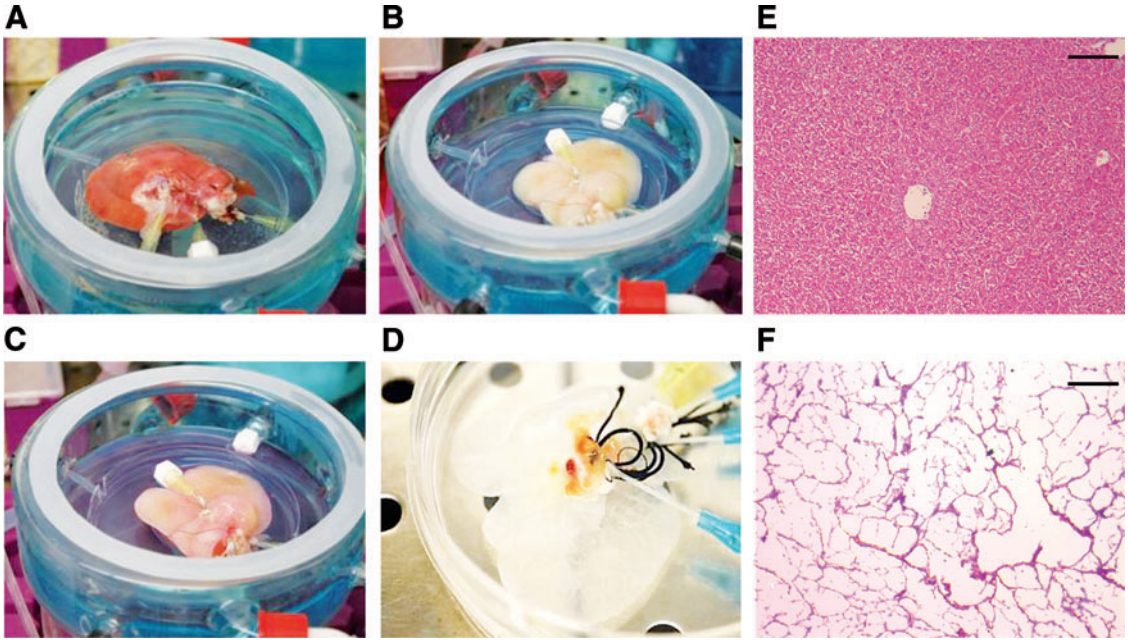

FIG. 1. *Ex vivo* decellularization of whole rat livers. Macroscopic appearance of the liver during different phases of decellularization **(A–C)**. Translucent structures were obtained at the end of the process **(D)** and it is possible to identify a network of tubular structures derived from the remnants of vessel and biliary duct systems. Representative micrographs of hematoxylin and eosin (H&E) staining of normal **(E)** and decellularized liver tissues **(F)** showing that after decellularization, a fine extracellular matrix (ECM) network was conserved, with the absence of cellular components. Scale bar = 100 μm. Color images available online at www.liebertpub.com/tea

revealed that after 21 days in culture, 13% of the cells were apoptotic in the bioscaffolds cultured in basal conditions (hepatocyte like). The viability rate was significantly improved when the HLSC-CM was added (2.8% of apoptotic cells). A similar effect was observed when recellularized bioscaffolds were stimulated with EGF and FGF (hepatocyte like + GF; 2.5% of apoptotic cells).

Considering that the HLSC have a high degree of proliferation, we explored at the end of the experiment, if this capability was modified by the direct interaction with the ECM.

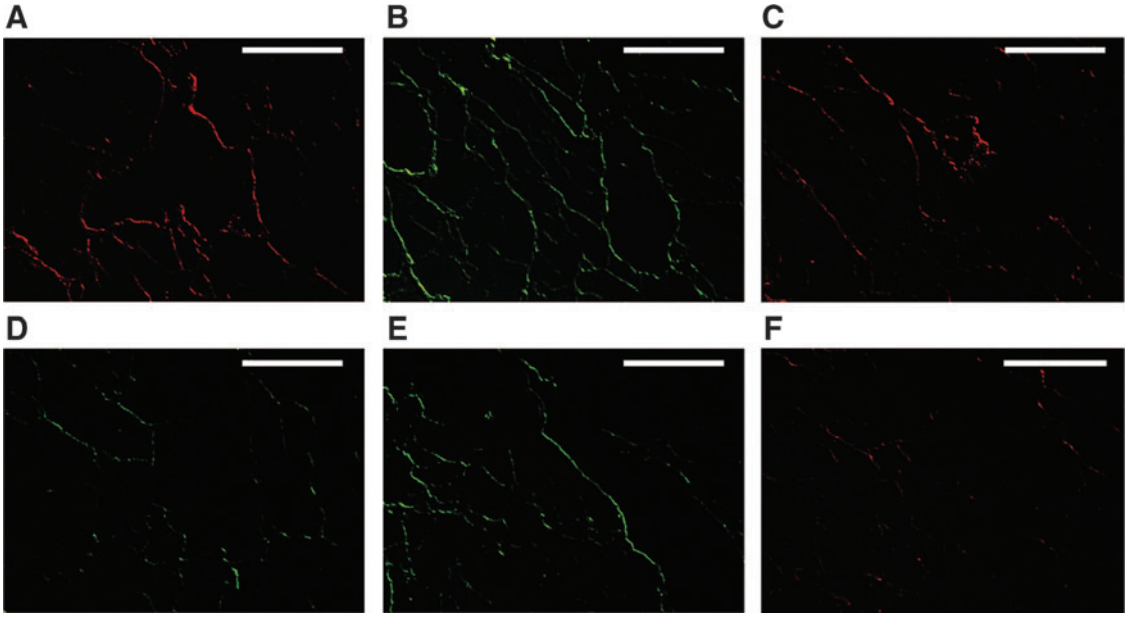

FIG. 2. Representative micrographs of immunofluorescence analysis of ECM proteins in acellular rat liver bioscaffolds. After decellularization, the ECM proteins such as collagen IV **(A,** Texas Red labeled secondary antibody), fibronectin **(B,** green Alexa Fluor labeled secondary antibody), actin **(C,** Texas Red labeled secondary antibody), laminin **(D,** green Alexa Fluor labeled secondary antibody), vimentin **(E,** green Alexa Fluor labeled secondary antibody), and cytokeratin 8–18 **(F)** were conserved. Scale bar = 100 μm.

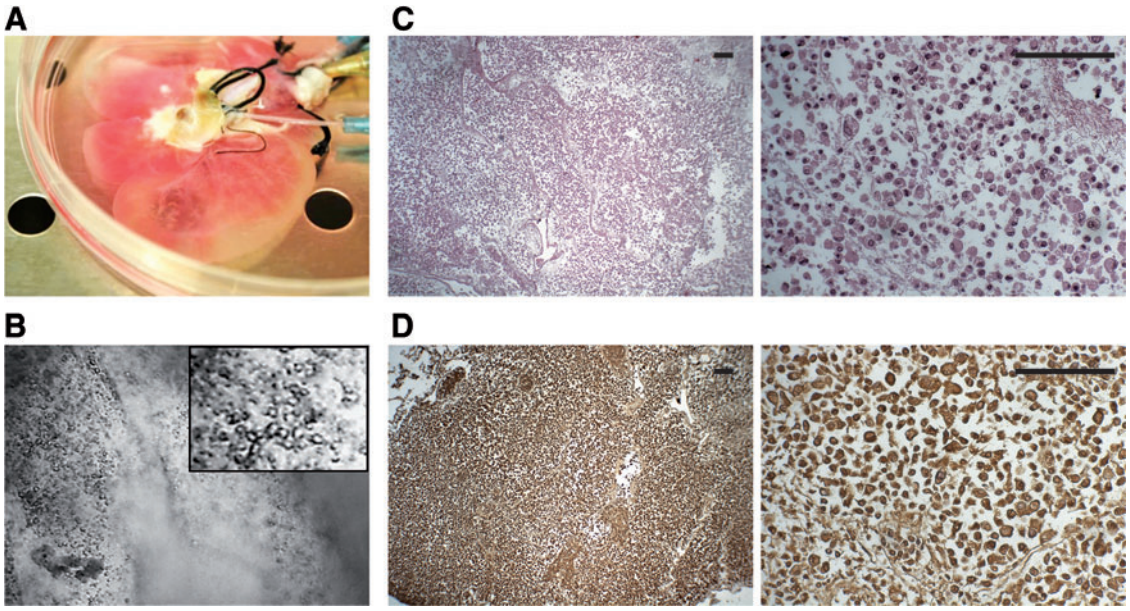

FIG. 3. Recellularization of acellular rat liver bioscaffolds with human liver stem-like cells (HLSC). The acellular bioscaffolds was perfused with α-MEM/EBM/FCS as a pretreatment 30 min before recellularization **(A)** and subsequently recellularized with HLSC (80×10^6 cells). The presence of cells into the bioscaffold was immediately confirmed by conventional microscopy **(B)**. Representative micrographs of H&E staining **(C)** showing the preservation of HLSC at the end of the experiment (21 days: original magnification ×40; inset: ×400), whereas the human origin of the cells was demonstrated by their positivity to HLA-1 **(D;** *brown* cells). Scale bar = 100 μm. HLA, human leucocyte antigen. Color images available online at www.liebertpub.com/tea

PCNA assay was performed to identify the cells in proliferation. The histological analysis demonstrated that in all the bioscaffolds, independently from the condition, a great majority of hepatocyte-like cells were negative to the PCNA indicating that cells lost their self-renewal capability (data not shown).

The histological analysis showed a major cell population characterized macroscopically by large cells with a central nucleus and granular cytoplasm that were attached to each other and dispersed through the entire bioscaffold (Fig. 3). This phenotype suggested the apparent differentiation of the

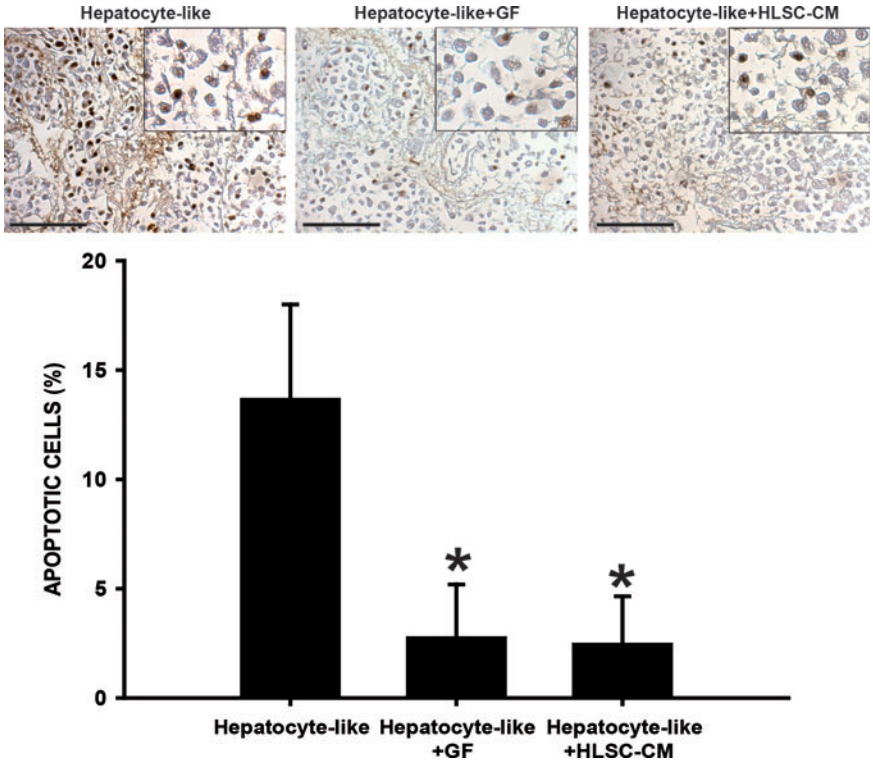

FIG. 4. Cell viability of bioscaffolds cultured for 21 days in different conditions. The TUNEL analysis demonstrated the presence of apoptotic cells independently of the culture condition. However, the quantitative analysis demonstrated that 13.7% of the cells fall in apoptosis when the bioscaffolds were cultured in standard conditions (hepatocyte like). The apoptotic rate was reduced when the HLSC-derived conditioned medium (HLSC-CM; Hepatocyte-like + HLSC-CM) or the epidermal growth factor–fibroblast growth factor (EGF-FGF; hepatocyte like + GF) were added to the medium (2.8% and 2.5%, respectively). Data are presented as the media of three independent experiments ± the standard error (SE). Original magnifications ×200; insets: ×400. *$p < 0.01$. Scale bar = 100 μm. Color images available online at www.liebertpub.com/tea

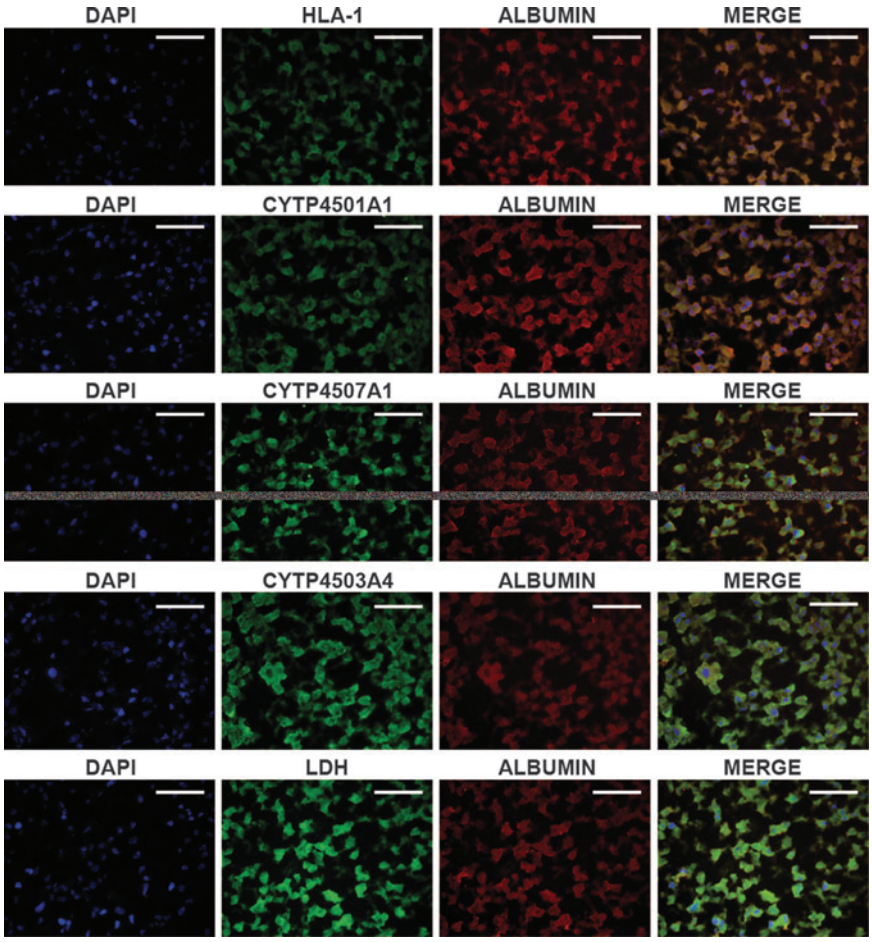

FIG. 5. Expression of human typical markers of mature hepatocytes in recellularized bioscaffolds. The immunofluorescence analysis demonstrated that after 21 days in culture, the hepatocyte-like cells (HLA^+) coexpressed albumin, lactate dehydrogenase (LDH), and three different subtypes of cytochrome P450 (1a1, 7a1, and 3a4), all of them typical markers of mature hepatocytes. Scale bar = 100 μm.

HLSC to hepatocyte-like cells. Differentiated hepatocyte-like cells lost their positivity to the embryonic cell markers, AFP, nestin, nanog, sox2, Musashi1, Oct 3/4, and pax2 (not shown) and acquired markers typical of mature cells. The immunocytochemistry analysis showed that a great majority of the cells were positive for human albumin and coexpressed the enzyme LDH and three different subclasses of the cytochrome P450 (Cyp450) (Fig. 5). These cells were also able to synthesize *de novo*, diverse human proteins of the ECM such as collagen IV, laminin, and fibronectin (Fig. 6). These were specific for human proteins and did not react with the rat ECM (Fig. 6; Neg Crtl). The expression of these proteins suggested that hepatocyte-like cells were able to humanize their environment, substituting the rat native matrix with the human homologous. This deposit of human matrix proteins was observed in all the

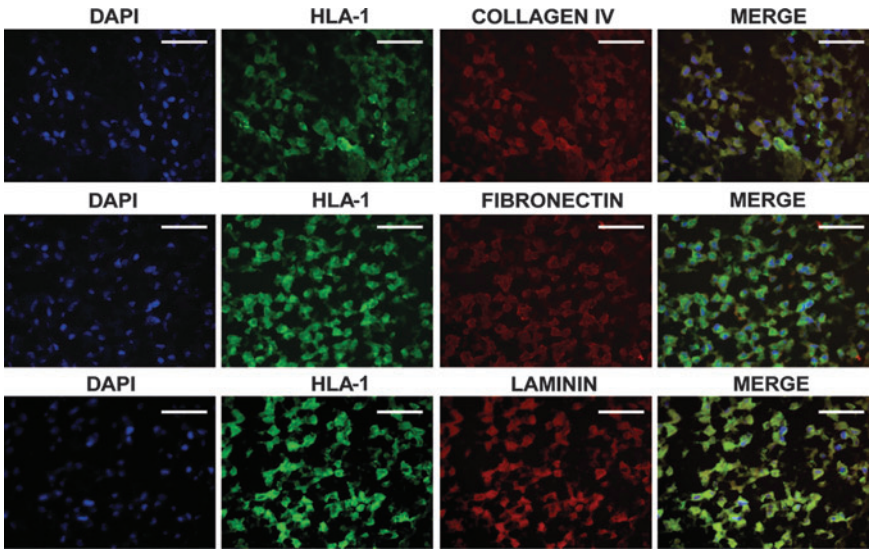

FIG. 6. Immunohistochemical characterization of human ECM proteins in recellularized bioscaffolds. After 21 days in culture, the HLSC ($albumin^+$ cells) were able to synthesize *de novo*, typical human ECM proteins such as collagen IV, fibronectin, and laminin. Scale bar = 100 μm.

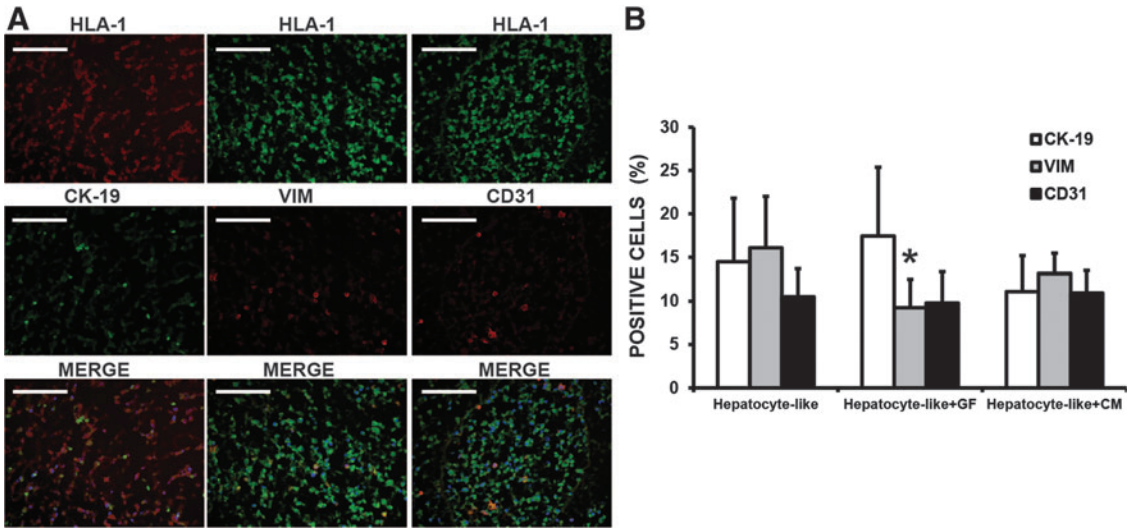

FIG. 7. The presence of epithelial- and endothelial-like cells in recellularized bioscaffolds. **(A)** Representative micrographs of immunofluorescence analysis demonstrating the presence of cytokeratin 19, vimentin, and CD31$^+$ cells. **(B)** The quantitative analysis demonstrated that cytokeratin 19$^+$, vimentin$^+$, and CD31$^+$ cells represent 14.5%, 16.1%, and 10.5% of the total cells, respectively. The addition of FGF-EGF (hepatocyte like + GF) reduced the percentage of vimentin$^+$ cells (9.2%), whereas no changes were observed when the HLSC-CM was added to the culture medium (hepatocyte-like + HLSC-CM). The other subpopulations (cytokeratin 19$^+$ and CD31$^+$) did not differ between treatments. Data are presented as the media of three different experiments ± standard deviation. *$p < 0.05$. Scale bar = 100 μm.

recellularized bioscaffolds independently of the treatment (data not shown).

In addition to the major population (hepatocyte like), we identified a second population forming small groups of cells dispersed through the entire bioscaffold. This population was constituted by two different subpopulations differing for the expression of specific cell markers (Fig. 7A). The first subpopulation was formed by cytokeratin 19-expressing cells (14.5%), whereas the other subpopulation expressed vimentin (16.1%) or CD31 (10.5%). The presence of cells expressing these markers suggests the generation of epithelial and endothelial lineages from the HLSC. The quantitative analysis showed that a percentage of the vimentin-positive cells had a tendency to be reduced in the scaffolds cultivated in the presence of FGF-EGF (hepatocyte like + GF, 9.2%) or in a medium enriched with HLSC-CM (hepatocyte like + HLSC-CM, 13.2%), whereas the other two subpopulations were not affected (Fig. 7).

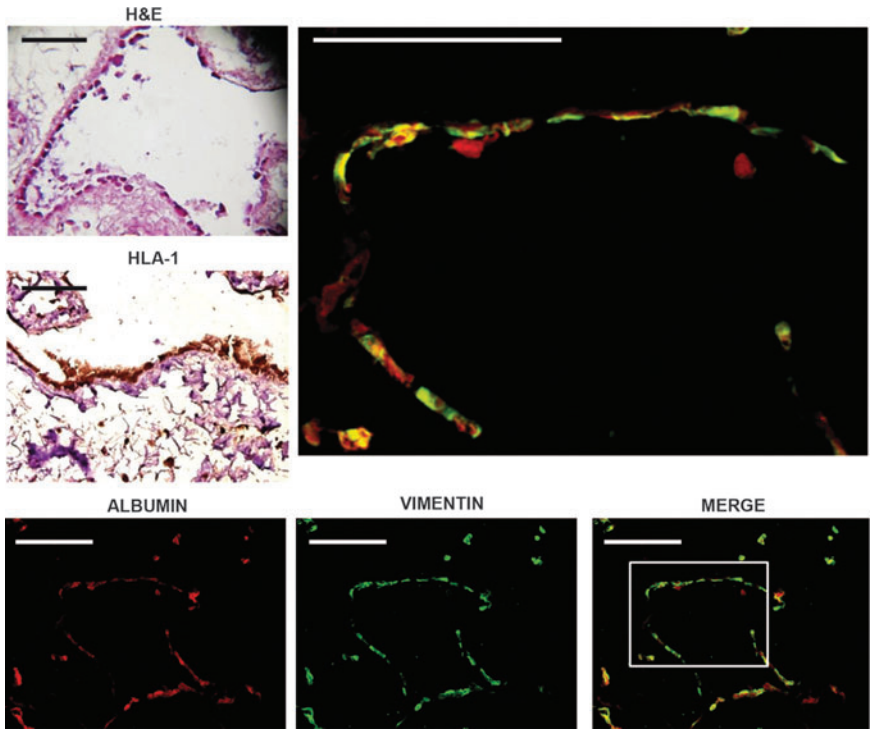

FIG. 8. Representative micrographs of endothelial-like cells forming tubular structures. H&E staining showing more *square-shaped* hepatocyte-like cells (HLA; *brown* cells) that were observed lining each other in a continuous monolayer forming tubular structures. Some cells expressing albumin were negative to vimentin.

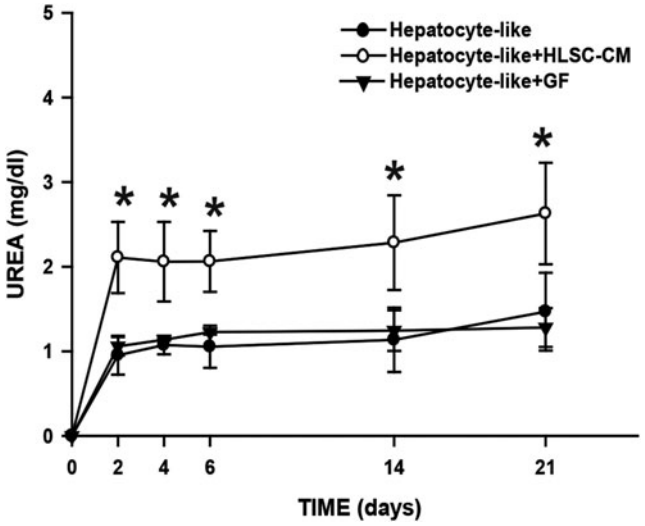

FIG. 9. Hepatocyte-like cells are metabolically active. The urea nitrogen is detected just 2 days after recellularization. In most conditions, the levels were maintained during the entire experiment ($\sim$1 mg/dL). The addition of HLSC-CM (hepatocyte-like + HLSC-CM) improved the metabolic activity of the cells, because the levels of urea nitrogen were $\sim$2-fold higher (2–2.5 mg/dL) when compared with the other conditions. Standard culture medium (see Materials and Methods section) was used as blank in the normalization and also represents the levels of blood urea nitrogen at time 0. Data are presented as the media of three independent experiments ± SE. $*p < 0.01$ with respect to the other three conditions.

The presence of vimentin$^+$ and CD31$^+$ cells suggested a possible neoangiogenesis derived from this cell subpopulation. As shown in Figure 8, we observed elongated and square-shaped cells forming a continuous monolayer contiguous or close to some tubular structures. Coexpression of albumin with the endothelial markers vimentin and CD31 indicated an immature phenotype of these cells. Cells nonadherent to ECMs were negative for vimentin and CD31. The presence of these double-positive cells attached to the matrix of remnant tubular structures suggested the importance of a direct modulation exerted by ECMs in guiding the HLSC-specific cell commitment.

To evaluate the metabolic activity of the hepatocyte-like population, the culture medium was collected at different experimental times (2, 4, 6, 14 and 21 days) and the urea nitrogen synthesis was assessed. Hepatocyte-like cells produced urea detectable already after 2 days from seeding HLSC in the acellular bioscaffolds (Fig. 9). In standard conditions, hepatocyte-like cells were able to produce $\sim$1 mg/dL and this concentration was maintained during the entire experiment. The production of urea was significantly increased up to 2–2.5 mg/dL, when recellularized bioscaffolds were cultured in the presence of the HLSC-CM (hepatocyte-like + HLSC-CM), whereas no major differences were observed in hepatocyte-like + GF bioscaffolds.

Discussion

The liver is able to regenerate itself maintaining an adequate volume and function. When the liver is undergoing up to 70% of resection, the restoration of the liver mass is carried out by the proliferation of hepatocytes and/or progenitors.[32,33] After an acute injury, the regenerative capacity of the liver is enough to maintain, temporally, the function of the organ. However, this effect is limited, especially in chronic or fulminant diseases, where the regenerative capacity of remnant resident cells is not enough to restore the normal anatomy and function of the organ, making orthotopic liver transplantation mandatory.

In this work, we were able to generate functional humanized livers using HLSC in combination with rat acellular liver bioscaffolds. The tridimensional structure of the native matrix and the preservation of bioactive molecules promoted differentiation and maturation of HLSC to functional hepatocytes. In addition, subgroups of cells were differentiated to endothelial-like or epithelial-like cells, suggesting that HLSC could participate also in the regeneration of both vascular and biliary systems when seeded in acellular natural bioscaffolds. Pluripotency of HLSC, including the ability to differentiate in endothelial cells, was as previously shown.[14]

Expression of the drug-metabolizing enzymes such as Cyp450 is commonly used as markers of hepatocyte differentiation.[14,34] The histological analysis made evident the expression of three types of CytP450 (1a1, 3a4, and 7a1) by the HLSC at the end of the experiments (21 days).

The hepatocytes control the homeostasis of fuel molecules such as glucose, glycogen, triglycerides, cholesterol, bile acids, and vitamins; metabolize amino acids and endogenous compounds such as heme and bilirubin; and are also responsible of the systemic ammonia detoxification in connection with urea synthesis, maintaining the ammonia and bicarbonate homeostasis under physiologic and pathologic conditions.[35] In our experiments, we observed the production of urea nitrogen in the medium of the recellularized bioscaffolds, detectable after 2 days in culture and maintained up to day 21 (Fig. 6). A significant increase in the metabolic activity was observed in the hepatocyte-like + HLSC-CM bioscaffolds, indicating that factors secreted by the cells have important trophic effects on the differentiation of HLSC.

Even if the ECM constitutes less than 3% of the liver tissue, it is formed by diverse proteins, which are organized in a tissue-specific arrangement, composed by collagens, laminins, proteoglycans, glycosaminoglycans, elastins, and other proteins. Physiologically, the ECM not only provides the architecture of tissues but also participates in cellular adhesion, migration, patterning, and phenotype.[36] Thus, the content of the diverse proteins forming the ECM seems to be important to maintain the differentiated functions in each individual cellular compartment of the liver.[29] Due to the high complexity of the ECM *in vivo*, it is difficult to construct synthetic scaffolds mimicking their natural composition as well as its microarchitecture that are able to support the hepatocyte survival and function when transplanted in rats. Baptista *et al.* demonstrated that decellularized liver matrix favor colonization of human fetal liver cells and human umbilical vein endothelial cells,[37]confirming the potentiality of bioscaffolds to be used in regenerative medicine for clinical applications. The natural matrices, due to the lack of immunogenicity, represent a potential alternative in tissue regeneration.[38] Barakat *et al.* described the capacity of acellular liver bioscaffolds to support and induce phenotypic maturation of human fetal hepatocytes,

demonstrating the possibility to use recellularized natural bioscaffolds in xenotransplantation therapies to replace or supplement allotransplantation.[39] The use of embryonic or fetal tissues is limited not only by the number of donors but also by the ethical and legal reasons.

Uygun *et al.* demonstrated that acellular bioscaffolds obtained from ischemic rat livers supported the efficient engraftment and function of adult primary hepatocytes.[40] This study served as proof-of-concept for generation of recellularized liver, but the use of xenogenic matrix would be limited by immunogenicity. Based on this observation, the authors suggested that organs derived from deceased donors, unsuitable for transplantation, could be used for fabrication of acellular human liver bioscaffolds. However, a limitation of this approach is the need of a large amount of normal human hepatocytes. The novelty of our approach is that the use of HLSC can be easy expanded in culture at variance of normal adult hepatocytes and could be used to recellularize the liver from deceased donors. Moreover, these experiments add new information on the differentiation capabilities of HLSC, which have been recently designed as ''Orphan Drug'' by the European Medical Agency for urea cycle disorders (EU/3/12/971; EU/3/11/904) and acute liver failure (EU/3/12/983). HLSC are easily obtainable from small surgical samples or from biopsies of human adult liver.[14,16] In addition, these cells exhibit a great proliferation potential, remain stable for over 30 culture passages, without chromosomal aberrations, and a good manufacturing protocol.

In conclusion, this work demonstrated that HLSC can be expanded satisfactorily and differentiated to functional hepatocyte-like cells and epithelial and endothelial cells when seeded in liver acellular scaffolds.

Acknowledgments

We thank Chiara Pasquino and Sara Previdi for their participation in fluorescence analysis and Federica Antico for providing technical assistance. This study was supported by the Fresenius Medical Care. Transparency declarations: C.T., V.N.T, F.F., and M.B.H.S. (Fresenius Medical Care) are employed by a commercial company and contributed to the study as researchers. M.B.H.S., C.T., and G.C. are named inventors in related patents.

Disclosure Statement

No competing financial interests exist.

References

1. Riordan, S.M., and Williams R. Use and validation of selection criteria for liver transplantation in acute liver failure. Liver Transpl **6,** 170, 2000.
2. Tolosa, L., Pareja-Ibars, E., Donato, M.T., Cortes, M., Lopez, S., Jimenez, N., Mir, J., Castell, J.V., and Gomez-Lechon, M.J. Neonatal livers: a source of good-performing hepatocytes for cell transplantation. Cell Transplant **23,** 1229, 2014.
3. Miyashita, H., Suzuki, A., Fukao, K., Nakauchi, H., and Taniguchi, H. Evidence for hepatocyte differentiation from embryonic stem cells in vitro. Cell Transplant **11,** 429, 2002.
4. Yamamoto, H., Quinn, G., Asari, A., Yamanokuchi, H., Teratani, T., Terada, M., and Ochiya, T. Differentiation of embryonic stem cells into hepatocytes: biological functions and therapeutic application. Hepatology **37,** 983, 2003.
5. Teramoto, K., Asahina, K., Kumashiro, Y., Kakinuma, S., Chinzei, R., Shimizu-Saito, K., Tanaka, Y., Teraoka, H., and Arii, S. Hepatocyte differentiation from embryonic stem cells and umbilical cord blood cells. J Hepatobiliary Pancreat Surg **12,** 196, 2005.
6. Teramoto, K., Hara, Y., Kumashiro, Y., Chinzei, R., Tanaka, Y., Shimizu-Saito, K., Asahina, K., Teraoka, H., and Arii, S. Teratoma formation and hepatocyte differentiation in mouse liver transplanted with mouse embryonic stem cell-derived embryoid bodies. Transplant Proc **37,** 285, 2005.
7. Cantz, T., Sharma, A.D., Jochheim-Richter, A., Arseniev, L., Klein, C., Manns, M.P., and Ott, M., Reevaluation of bone marrow-derived cells as a source for hepatocyte regeneration. Cell Transplant **13,** 659, 2004.
8. Kanazawa, Y., and Verma, I.M. Little evidence of bone marrow-derived hepatocytes in the replacement of injured liver. Proc Natl Acad Sci U S A **100(Suppl 1),** 11850, 2003.
9. Alison, M.R., Poulsom, R., Jeffery, R., Dhillon, A.P., Quaglia, A., Jacob, J., Novelli, M., Prentice, G., Williamson, J., and Wright, N.A. Hepatocytes from non-hepatic adult stem cells. Nature **406,** 257, 2000.
10. Theise, N.D., Badve, S., Saxena, R., Henegariu, O., Sell, S., Crawford, J.M., and Krause, D.S. Derivation of hepatocytes from bone marrow cells in mice after radiation-induced myeloablation. Hepatology **31,** 235, 2000.
11. Theise, N.D., Nimmakayalu, M., Gardner, R., Illei, P.B., Morgan, G., Teperman, L., Henegariu, O., and Krause, D.S. Liver from bone marrow in humans. Hepatology **32,** 11, 2000.
12. Lagasse, E., Connors, H., Al-Dhalimy, M., Reitsma, M., Dohse, M., Osborne, L., Wang, X., Finegold, M., Weissman, I.L., and Grompe, M. Purified hematopoietic stem cells can differentiate into hepatocytes in vivo. Nat Med **6,** 1229, 2000.
13. Petersen, B.E., Bowen, W.C., Patrene, K.D., Mars, W.M., Sullivan, A.K., Murase, N., Boggs, S.S., Greenberger, J.S., and Goff, J.P. Bone marrow as a potential source of hepatic oval cells. Science **284,** 1168, 1999.
14. Herrera, M.B., Bruno, S., Buttiglieri, S., Tetta, C., Gatti, S., Deregibus, M.C., Bussolati, B., and Camussi, G. Isolation and characterization of a stem cell population from adult human liver. Stem Cells **24,** 2840, 2006.
15. Sokal, E.M. From hepatocytes to stem and progenitor cells for liver regenerative medicine: advances and clinical perspectives. Cell Prolif **44(Suppl 1),** 39, 2011.
16. Herrera, M.B., Fonsato, V., Bruno, S., Grange, C., Gilbo, N., Romagnoli, R., Tetta, C., and Camussi, G. Human liver stem cells improve liver injury in a model of fulminant liver failure. Hepatology **57,** 311, 2013.
17. De Coppi, P., Delo, D., Farrugia, L., Udompanyanan, K., Yoo, J.J., Nomi, M., Atala, A., and Soker, S. Angiogenic gene-modified muscle cells for enhancement of tissue formation. Tissue Eng **11,** 1034, 2005.
18. Hollister, S.J. Porous scaffold design for tissue engineering. Nat Mater **4,** 518, 2005.
19. Levenberg, S., Rouwkema, J., Macdonald, M., Garfein, E.S., Kohane, D.S., Darland, D.C., Marini, R., van Blitterswijk, C.A., Mulligan, R.C., D'Amore, P.A., and Langer,

R. Engineering vascularized skeletal muscle tissue. Nat Biotechnol **23,** 879, 2005.
20. Kaihara, S., Borenstein, J., Koka, R., Lalan, S., Ochoa, E.R., Ravens, M., Pien, H., Cunningham, B., and Vacanti, J.P. Silicon micromachining to tissue engineer branched vascular channels for liver fabrication. Tissue Eng **6,** 105, 2000.
21. Griffith, C.K., Miller, C., Sainson, R.C., Calvert, J.W., Jeon, N.L., Hughes, C.C., and George, S.C. Diffusion limits of an in vitro thick prevascularized tissue. Tissue Eng **11,** 257, 2005
22. Gilmore, L., Rimmer, S., McArthur, S.L., Mittar, S., Sun, D., and Macneil, S. Arginine functionalization of hydrogels for heparin binding-a supramolecular approach to developing a pro-angiogenic biomaterial. Biotechnol Bioeng **110,** 296, 2013.
23. Oliviero, O., Ventre, M., and Netti, P.A. Functional porous hydrogels to study angiogenesis under the effect of controlled release of vascular endothelial growth factor. Acta Biomater **8,** 3294, 2012.
24. Zou, D., Zhang, Z., He, J., Zhang, K., Ye, D., Han, W., Zhou, J., Wang, Y., Li, Q., Liu, X., Zhang, X., Wang, S., Hu, J., Zhu, C., Zhang, W., Zhou, Y., Fu, H., Huang, Y., and Jiang, X. Blood vessel formation in the tissue-engineered bone with the constitutively active form of HIF-1α mediated BMSCs. Biomaterials **33,** 2097, 2012.
25. Xiao, C., Zhou, H., Liu, G., Zhang, P., Fu, Y., Gu, P., Hou, H., Tang, T., and Fan, X. Bone marrow stromal cells with a combined expression of BMP-2 and VEGF-165 enhanced bone regeneration. Biomed Mater **6,** 015013, 2011.
26. Singh, S., Wu, B.M., and Dunn, J.C. Delivery of VEGF using collagen-coated polycaprolactone scaffolds stimulates angiogenesis. J Biomed Mater Res A **100,** 720, 2012.
27. Shupe, T., Williams, M., Brown, A., Willenberg, B., and Petersen, B.E. Method for the decellularization of intact rat liver. Organogenesis **6,** 134, 2010.
28. Meredith, J.E., Jr., Fazeli, B., and Schwartz, M.A. The extracellular matrix as a cell survival factor. Mol Biol Cell **4,** 953, 1993.
29. Schuppan, D., Ruehl, M., Somasundaram, R., and Hahn, E.G. Matrix as a modulator of hepatic fibrogenesis. Semin Liver Dis **21,** 351, 2001.
30. Cavallari, C., Fonsato, V., Herrera, M.B., Bruno, S., Tetta, C., and Camussi, G. Role of Lefty in the anti tumor activity of human adult liver stem cells. Oncogene **32,** 819, 2013.
31. Fonsato, V., Collino, F., Herrera, M.B., Cavallari, C., Deregibus, M.C., Cisterna, B., Bruno, S., Romagnoli, R., Salizzoni, M., Tetta, C., and Camussi, G. Human liver stem cell-derived microvesicles inhibit hepatoma growth in SCID mice by delivering antitumor microRNAs. Stem Cells **30,** 1985, 2012.
32. Cardinale, V., Wang, Y., Carpino, G., Cui, C.B., Gatto, M., Rossi, M., Berloco, P.B., Cantafora, A., Wauthier, E., Furth, M.E., Inverardi, L., Dominguez-Bendala, J., Ricordi, C., Gerber, D., Gaudio, E., Alvaro, D., and Reid, L. Multipotent stem/progenitor cells in human biliary tree give rise to hepatocytes, cholangiocytes, and pancreatic islets. Hepatology **54,** 2159, 2011.
33. Turner, R., Lozoya, O., Wang, Y., Cardinale, V., Gaudio, E., Alpini, G., Mendel, G., Wauthier, E., Barbier, C., Alvaro, D., and Reid, L.M. Human hepatic stem cell and maturational liver lineage biology. Hepatology 53, 1035, 2011.
34. Rhodes, S.P., Otten, J.N., Hingorani, G.P., Hartley, D.P., and Franklin, R.B. Simultaneous assessment of cytochrome P450 activity in cultured human hepatocytes for compound-mediated induction of CYP3A4, CYP2B6, and CYP1A2. J Pharmacol Toxicol Methods **63,** 223, 2011.
35. Guyton, A.C., and Hall, J.E. The liver as an organ. In: Guyton, A.C., and Hall, J.E., eds. Textbook of Medical Physiology. Philadelphia, PA: Elsevier Masson, 2010, pp. 859–864.
36. Schuppan, D., and Rühl, M. Matrix in signal transduction and growth factor modulation. Braz J Med Biol Res **27,** 2125, 1994.
37. Baptista, P.M., Siddiqui, M.M., Lozier, G., Rodriguez, S.R., Atala, A., and Soker, S. The use of whole organ decellularization for the generation of a vascularized liver organoid. Hepatology **53,** 604, 2011.
38. Yang, L.M., Liu, X.L., Zhu, Q.T., Zhang, Y., Xi, T.F., Hu, J., He, C.F., and Jiang, L. Human peripheral nerve-derived scaffold for tissue-engineered nerve grafts: histology and biocompatibility analysis. J Biomed Mater Res B Appl Biomater, **96,** 25, 2011.
39. Barakat, O., Abbasi, S., Rodriguez, G., Rios, J., Wood, R.P., Ozaki, C., Holley, L.S., and Gauthier, P.K. Use of decellularized porcine liver for engineering humanized liver organ. J Surg Res **173,** e11, 2012.
40. Uygun, B. E., Soto-Gutierrez, A., Yagi, H., Izamis, M.L., Guzzardi, M.A., Shulman, C., Milwid, J., Kobayashi, N., Tilles, A., Berthiaume, F., Hertl, M., Nahmias, Y., Yarmush, M.L., and Uygun, K. Organ reengineering through development of transplantable recellularized liver graft using decellularized liver matrix. Nat Med **16,** 814, 2010.

Address correspondence to:
Giovanni Camussi, MD, PhD
Department of Medical Sciences
University of Torino
Corso Dogliotti 14
Torino 10126
Italy

E-mail: giovanni.camussi@unito.it

Received: October 3, 2014
Accepted: March 16, 2015
Online Publication Date: April 28, 2015